Available online at www.sciencedirect.com
ScienceDirect
Journal of Molecular Catalysis A: Chemical 258 (2006) 89–94
JOURNAL OF MOLECULAR CATALYSIS A: CHEMICAL
www.elsevier.com/locate/molcata

Ullmann coupling reaction in aqueous conditions over the Ph-MCM-41 supported Pd catalyst

Ying Wan, Jia Chen, Dieqing Zhang, Hexing Li *

Department of Chemistry, Shanghai Normal University, Shanghai 200234, China

Received 16 December 2005; received in revised form 7 May 2006; accepted 9 May 2006
Available online 19 June 2006

Abstract

Functionalized MCM-41 samples containing different contents of phenyl groups (Ph-MCM-41) were synthesized by co-condensation of phenyltrimethoxysilane (PTMS) and tetraethyl orthosilicate (TEOS) at room temperature. These Ph-MCM-41 samples still exhibited the ordered mesoporous structure even at the Ph-content up to 20% and after depositing Pd particles to form the Pd/Ph-MCM-41 catalyst. For the iodobenzene Ullmann coupling reaction in aqueous conditions, Pd/Ph-MCM-41 exhibited much higher activity and selectivity toward biphenyl than Pd/SiO_2 and Pd/MCM-41. The conversion reached 75.4% after 10 h at 100 °C and the selectivity remained 98%. In addition, the Pd/Ph-MCM-41 catalyst was able to be used atleast three times with only a slight decrease in both activity and selectivity. The results show good potential of this kind of catalyst for industrial application in viewpoint of green chemistry since the replacement of organic solvent with water could greatly reduce the environmental pollution. According to various characterizations, such as XRD, TEM, NMR, N_2 adsorption–desorption isotherms, the excellent activity and selectivity of the Pd/Ph-MCM-41 could be attributed to the high surface area of Ph-MCM-41 which ensured the high and uniform dispersion of Pd particles, the ordered mesoporous structure which facilitated the diffusion of reactant and product molecules, the increase in hydrophobicity of the catalyst owing to the Ph-modification which favored the entrance of reactant molecules into the channels to have contact with Pd active sites and also inhibited the dehalogenation of iodobenzene to form benzene.

Keywords: Green chemistry; Pd/Ph-MCM-41; Iodobenzene (Ar-I); Ullmann reaction; H_2O medium

1. Introduction

The iodobenzene (Ar-I) coupling reaction (Ullmann reaction) has been widely used for synthesizing aromatic compounds for fine chemical, agrochemical, and pharmaceutical applications [1,2]. In industry, the synthesis is usually carried out in anhydrous solvents. The use of large amount of organic solvents for reaction and product isolation eventually causes environmental problems because volatile organic compounds are a principal cause of industrial pollution. In viewpoint of green chemistry, the Ullmann reaction carried out in aqueous conditions should be more environmentally friendly since water could be considered as the most innocuous substance on earth and therefore the safest solvent. Up to now, most studies are focused on homogeneous catalysts in the presence of phase-transfer catalysts due to solubility limitation of organic substances in water [3,4]. Generally, heterogeneous catalysts are superior to homogeneous catalysts owing to their easy separation from the products. Meanwhile, the heterogeneous catalysts can be used repetitively, which may reduce the catalyst cost. However, their low activity and/or selectivity seems a problem [5,6]. Mesoporous materials usually exhibited high surface area and large pore size [7,8]. Depositing the metallic particles on the supports with mesoporous structure may ensure the high dispersion of active sites and facilitate the diffusion of reactant molecules. Meanwhile, the enrichment of OH groups on the mesoporous materials makes it possible to modify the inorganic supports with organic groups on the outer surface and pore surface, which could improve surface chemistry of the catalysts, such as the acidic–basic property, the hydrophilic–hydrophobic property, etc. [9–14], and thus, could promote chemical reactions, especially the organic synthetic reactions carried out in water. In this paper, we report a new Pd/Ph-MCM-41 catalyst with the Ph-functionalized MCM-41 (Ph-MCM-41) as the support. Its catalytic performance in

* Corresponding author. Tel.: +86 21 64322272; fax: +86 21 64322272.
E-mail address: hexing-li@shnu.edu.cn (H. Li).

1381-1169/$ – see front matter © 2006 Elsevier B.V. All rights reserved.
doi:10.1016/j.molcata.2006.05.018

Ullmann reaction was examined and the correlation between catalytic properties and structural characteristics are discussed briefly based on various characterizations.

2. Experimental

2.1. Catalyst preparation

The Ph-modified MCM-41 sample (Ph-MCM-41) was prepared by co-condensation of phenyltrimethoxysilane (PTMS) and tetraethyl orthosilicate (TEOS) as mixed silicon sources. In a typical synthesis, 0.05 mol of PTMS and TEOS mixture with a given molar ratio were mixed with 108 ml aqueous solution containing 2.4 g cetyl(hexadecyl)trimethylammonioum bromide (CTMABr) and 1.0 M NaOH and then the mixture was stirred for 48 h at room temperature. After being filtrated out and dried in vacuum at 80 °C for 10 h, the solid was treated with 1.0 M HCl ethanol solution to remove the surfactant template and other organic residues. The resultant Ph-MCM-41 was washed thoroughly and dried in vacuum for another 10 h. The Ph-content in the Ph-MCM-41 was adjusted by changing the molar ratio of PTMS/TEOS (x:y) in the initial mixture. The as-prepared samples were denoted by Ph-MCM-41 (x:y).

Pd/Ph-MCM-41 catalysts were prepared by impregnating the as-prepared Ph-MCM-41 with $PdCl_2$ dilute solution containing 1.67 wt.% Pd at room temperature for 24 h. After being dried at 100 °C, the supported Pd(II) species were reduced by 10% H_2/N_2 at 200 °C for 3 h.

2.2. Characterization

Small-angle X-ray diffraction (XRD) measurements were performed on a Rigaku D/maxrB diffractometer with Cu Kα X-ray. N_2 adsorption–desorption isotherms were measured on a Quantachrome NOVA 4000e analyzer. Specific surface areas (S_{BET}) were calculated by using the multiple-point Brunauer–Emmett–Teller (BET) method in the relative pressure range of $P/P_0 = 0.05$–0.25. Pore size distribution curves were obtained based on the Barrett–Joyner–Halenda (BJH) model, from which the average pore size (d_P) and the pore volume (V_P) were also determined. Transmission electron microscopy (TEM) images were obtained on a JEOL JEM2011 electron microscope. X-ray photoelectron spectroscopy (XPS) measurements were performed on a Perkin-Elmer PHI 5000CESCA system with a base pressure of 10^{-9} Torr. All the binding energies were calibrated by using the contaminant carbon ($C_{1s} = 284.6$ eV) as a reference. FT-IR spectra were recorded with a Nicolet Magna 550 IR spectrometer. Temperature-programmed reduction (TPR) was conducted on a Quantachrome CHEMBET-3000 system, during which all the samples were pretreated with H_2 gas flow at room temperature for 2 h. ^{13}C MAS NMR and ^{29}Si MAS NMR spectra were recorded on a Bruker DRX-400 NMR spectrometer. The catalysts were analyzed using a Varian VISTA-MPX inductively coupled plasma optical emission spectrometer (ICP-OES) to determine the palladium contents.

2.3. Activity test

In a typical run of activity test, 4.46 mmol PhI, 10 ml distilled water, 0.5 g as-prepared catalyst with Pd loading of 6 wt.%, 1.1 g HCOONa as a reducing agent and 1.4 g KOH were mixed in a 50 ml round-bottomed flask. The mixture was vigorously stirred to minimize any diffusion effects. After refluxing at 100 °C for 10 h, the reaction mixture was filtrated and then extracted with toluene. The products were analyzed by a gas chromatograph (Agilent 1790) equipped with a JW DB-5, 95% dimethyl 1-(5%)-diphenylpolysiloxane column and an FID detector. The column temperature was programmed from 100 to 250 °C at the ramp speed of 15 °C/min. N_2 was used as carrier gas. All tests were repeated at least three times, and were found the experimental errors within ±5%. The solid catalyst was washed by toluene and re-used with fresh solvent and reactants for subsequent runs under the same reaction conditions.

3. Results and discussion

Fig. 1 shows the FTIR spectra of the as-prepared MCM-41 and the Ph-MCM-41 (1:4) samples. The Ph-MCM-41 (1:4) sample displayed absorbance peaks characteristic of MCM-41 [15] at 3500 cm^{-1} for ν(O–H), at 1474 cm^{-1} for δ(O–H), at 600 cm^{-1} for ω(O–H), at 1000–1300 cm^{-1} for ν_{as}(Si–O), and at 456 cm^{-1} for δ(Si–O), respectively. Besides, additional absorbance peaks were also found in the Ph-MCM-41. The peaks at 3100–3000 cm^{-1} and 690–740 cm^{-1} could be attributed to ν(C–H) and δ(C–H) in benzene ring, while the peaks at 1450–1460 cm^{-1} resulted from the framework vibration, i.e. ν(C–C) of the benzene ring. These results demonstrate the successful incorporation of the Ph-group in the wall of MCM-41 [15]. The peak corresponding to ν(Si–C) should appear at 1160–1170 cm^{-1}. However, it was difficult to be distinguished since it was overlapped by the peaks corresponding to ν_{as}(Si–O) in the network of MCM-41. In comparison with pure

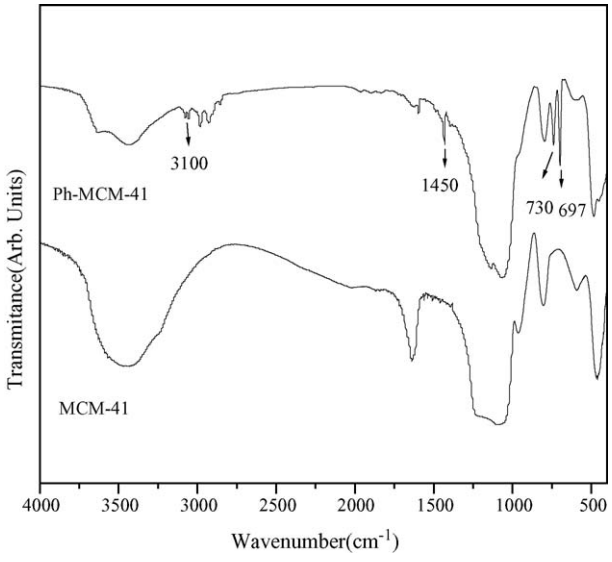

Fig. 1. FTIR spectra of MCM-41 and Ph-MCM-41 (1:4).

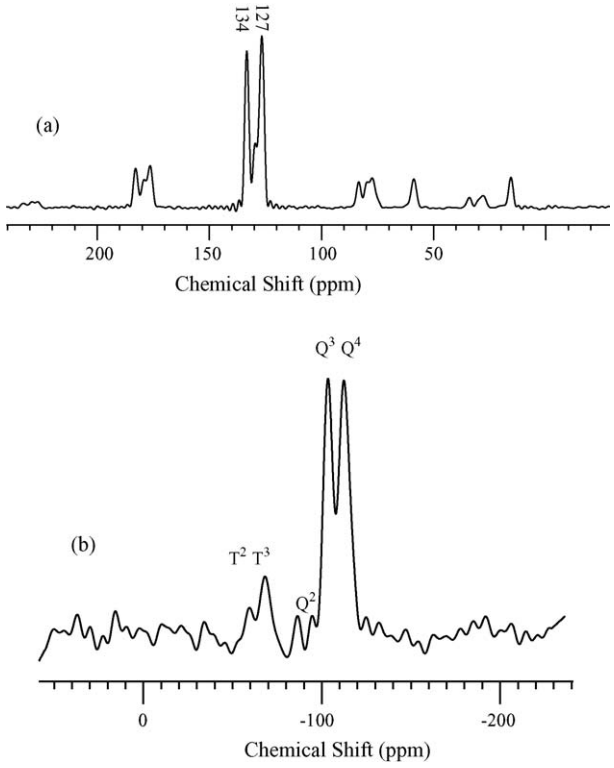

Fig. 2. (a) ^{13}C CP MAS and (b) ^{29}Si CP MAS NMR spectra of Ph-MCM-41 (1:4).

silica MCM-41, the intensity of the peak at 3100–3000 cm^{-1} decreased abruptly, possibly owing to the substitution of Ph groups for a large fraction of surface OH groups.

The incorporation of the Ph-group into the MCM-41 network could be further confirmed by solid-state NMR spectra. As shown in Fig. 2(a), the ^{29}Si MAS NMR spectra of Ph-MCM-41 (1:4) displayed three resonance peaks up-field corresponding to Q^4 ($\delta = -111$ ppm), Q^3 ($\delta = -102$ ppm), and Q^2 ($\delta = -91$ ppm), and two peaks down-field corresponding to T^3 ($\delta = -67$ ppm) and T^2 ($\delta = -58$ ppm), respectively [16,17]. Where $Q^n = Si(OSi)_n–(OH)_{4-n}$, $n = 2–4$ and $T^m = RSi(OSi)_m–(OH)_{3-m}$, $m = 1–3$ [18]. The presence of T^m peaks confirmed the incorporation of the organic silane moieties as a part of the silica wall structure. This was supported

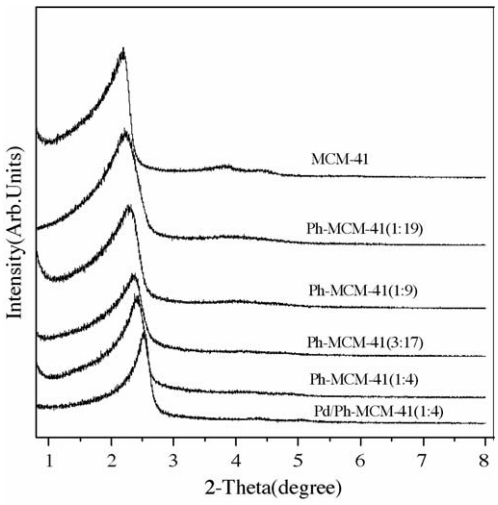

Fig. 4. Small-angle XRD patterns of pure silica MCM-41, Ph-MCM-41 with different Ph-contents, and 6 wt.% Pd/Ph-MCM-41 (1:4).

by the ^{13}C CPMAS NMR spectrum. As shown in Fig. 2(b), the Ph-MCM-41 sample clearly displayed two peaks around 134.9 and 127.5 ppm, corresponding to C atoms in the benzene ring, which was incorporated in the network of the SiO_2 [19]. The $T^m/(T^m + Q^n)$ ratio in the Ph-MCM-41 sample was estimated at 0.20, almost the same as the PTMS/(PTMS + TEOS) molar ratios in the initial mixture, suggesting that nearly all the PTMS molecules were co-condensed with the TEOS; i.e. the loss of PTMS during the co-condensation could be neglected.

As shown in Fig. 3, the TEM image demonstrated that Ph-MCM-41 (1:4) preserved the ordered hexagonal structure and that the Pd particles were distributed homogeneously in the pore channels of the Ph-MCM-41 support, resulting in a nanowire-like morphology. But the ordering degree decreased in comparison with pure silica MCM-41. The XRD patterns (see Fig. 4) also revealed that, like pure silica MCM-41, Ph-MCM-41 exhibited a strong peak corresponding to (1 0 0) diffraction around $2\theta = 1.6–3^\circ$ and weak peaks characteristic of (1 1 0) and (2 0 0) diffractions around $2\theta = 3–6^\circ$, indicating that the long-range ordered hexagonal mesoporous structure was retained [20]. The decrease in the peak intensity after Ph-modification suggested that the ordered mesoporous structure was partially damaged

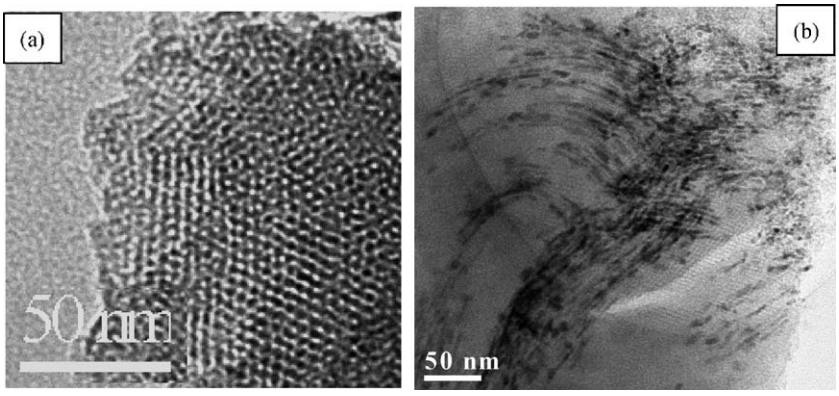

Fig. 3. TEM images of (a) Ph-MCM-41 (1:4) and (b) 6 wt.% Pd/Ph-MCM-41 (1:4).

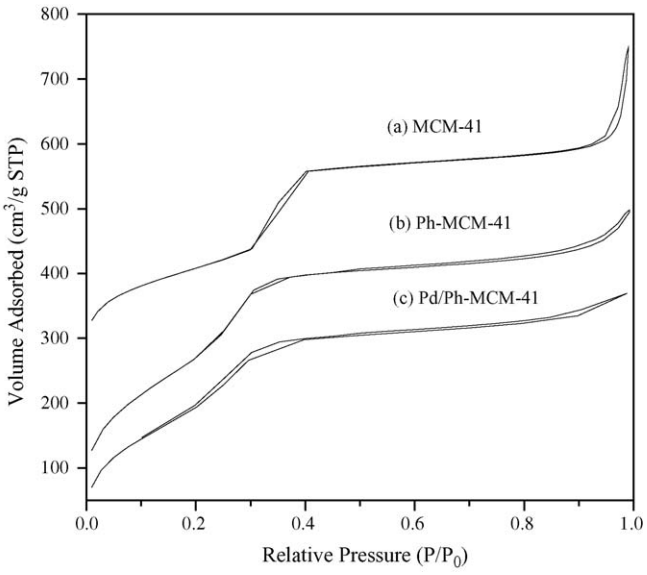

Fig. 5. N_2 adsorption–desorption isotherms of pure silica MCM-41, Ph-MCM-41 (1:4) and the 6 wt.% Pd/Ph-MCM-41 (1:4).

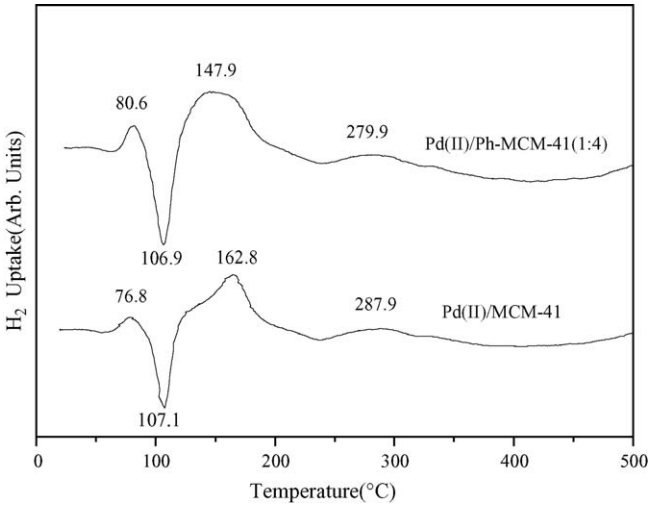

Fig. 6. TPR profile of the precursor of 6 wt.% Pd/Ph-MCM-41 (1:4).

since the interaction between the organic groups and the micelles may disturb the cooperative assembly of silica and CTMABr surfactant into highly ordered mesostructure [21]. The ordering degree of mesoporous structure decreased with the increase in the Ph-content and further decreased after being loaded with metallic Pd particles on the Ph-MCM-41 support. Meanwhile, the principal peak of the Ph-MCM-41 samples shifted to higher values with the increase in the Ph-content and the Pd deposition, indicating a decrease in basal (d_{100}) spacing [22].

Fig. 5 demonstrated that both Ph-MCM-41 and Pd/Ph-MCM-41 samples displayed typical IV type N_2 adsorption–desorption isotherms as found in pure silica MCM-41, which was attributed to the capillary condensation of N_2 in the mesopores [23]. Based on the N_2 adsorption–desorption isotherms, some structural parameters were calculated and listed in Table 1. One could see that the modification with the Ph-group slightly decreased the surface area (S_{BET}), the pore volume (V_P) and the pore size (d_P), possibly due to the coverage of the pore wall of the MCM-41 by the Ph-groups. These results were supported by the wall thickness calculated by using $a_0 - d_P$, where the lattice parameter $a_0 = 2d_{100}/\sqrt{3}$. From Table 1, it was clear that wall thickness slightly increased with the increase in the Ph-groups incorporated into MCM-41. Depositing Pd particles on the Ph-MCM-41support further decreased the S_{BET}, V_P and d_P, which could be easily understood by considering the occupation of Pd particles in the pore channels, corresponding to the increase in the pore wall thickness (see Table 1).

As shown in Fig. 6, the TPR profiles demonstrated that most Pd(II) species on the Ph-MCM-41 or the MCM-41 support were reduced readily to PdH_2 even at ambient temperature [24]. Only a small portion of the Pd(II) species (about 30%) was reduced at ~80 °C, which could be attributed to the stronger metal–support interaction between the Pd(II) and the support. A significant negative peak appeared around 106 °C owing to the decomposition of PdH_2. A broad peak around 280 °C could be attributed to hydrogen spillover [25] rather than the unreduced Pd(II) species. This was supported by XPS spectra. As shown in Fig. 7, only the metallic Pd species were observed, corresponding to the binding energies of 335.7 eV ($Pd_{3d5/2}$) and 340.8 eV in ($Pd_{3d1/2}$) [26], respectively, indicating the Pd(II) species deposited on the Ph-MCM-41 were completely reduced by 10% H_2/N_2 at 200 °C.

The Ullmann reaction was a well-documented reaction. Under the present conditions, only two products were identified during Ar-I Ullmann coupling reaction over different Pd-based supported catalysts. One is the target product biphenyl (Ar-Ar) which resulted from the coupling reaction of Ar-I. The other is the side-product benzene which resulted from dehalogenation of Ar-I to Ar-H. Thus, the reaction mechanism could be simply described as follows [25]:

Table 1
Structural parameters of different samples

Sample	d_{100} (nm)	S_{BET} (m^2/g)	V_P (cm^3/g)	d_P (nm)	Wall thickness (nm)
MCM-41	4.01	1242	0.90	3.6	1.0
Ph-MCM-41 (1:19)	3.96	1012	0.85	3.3	1.3
Ph-MCM-41 (1:9)	3.89	1006	0.77	2.7	1.8
Ph-MCM-41 (3:17)	3.72	1000	0.62	2.3	2.0
Ph-MCM-41 (1:4)	3.66	989	0.51	1.9	2.3
Ph-MCM-41 (3:7)	3.49	997	0.49	1.8	2.2
6 wt.% Pd/Ph-MCM-41 (1:4)	4.24	974	0.48	1.8	3.1

Pore wall thickness = a_0 − pore size, where a_0(lattice parameter) = $2d_{100}/\sqrt{3}$.

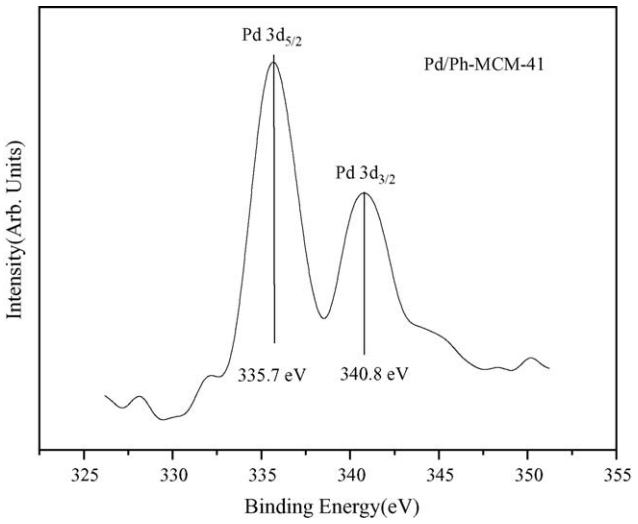

Fig. 7. XPS spectrum of 6 wt.% Pd/Ph-MCM-41 (1:4).

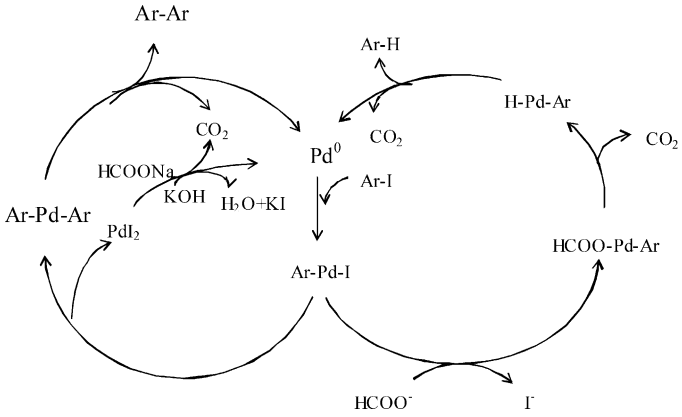

where HCOONa was used to reduce Pd(II) for regenerating the catalyst and KOH was used to neutralize the HX resulting from the reduction of PdX_2. Preliminary kinetic studies revealed that the increase in the stirring rate had no significant influence on the reaction rate. Meanwhile, the reaction rate increased nearly proportionally with increasing amount of Pd/Ph-MCM-41 catalyst. These results suggested that the diffusion effect on the reaction kinetics could be neglected under the present conditions. From Table 2, one could see that the increase in the reaction temperature enhanced the conversion. But the selectivity decreased abruptly when the reaction temperature increased from 100 to 120 °C. Meanwhile, although the conversion increased with the increase in reaction time, the selectivity to biphenyl decreased rapidly when the reaction time increased from 10 to 12 h. Thus, the optimum reaction conditions were reaction temperature = 100 °C and reaction time = 10 h.

As shown in Table 2, Pd/MCM-41 exhibited much higher activity and better selectivity to biphenyl than Pd/SiO_2, possibly owing to the higher surface area and mesoporous structure of the MCM-41, which increased the dispersion degree of Pd active sites and also facilitated the diffusion of Ar-I molecules in the channels to contact with the Pd active sites. Depositing the Pd particles on the Ph-MCM-41 support could further enhance the activity and the selectivity to biphenyl. Both the activity and the selectivity increased with the increase in the Ph-content incorporated into MCM-41. The promoting effect of the Ph-modification on the activity and selectivity could be attributed to the increase in the hydrophobicity of the outer surface and especially on the pore surface. On one hand, the hydrophobicity could facilitate the entrance of iodobenzene molecules into the channels of the catalyst and thus more iodobenzene molecules could make contact with Pd active sites easily, which may increase the activity. On the other hand, the hydrophobicity could also inhibit the entrance of water molecules into the channels, which may protect the pore walls from the attack of water [27]. The improvement of the hydrothermal stability may protect the mesoporous structure of the catalyst from collapse, which may retain the high dispersion of Pd particles on the support and also facilitate the diffusion of reactant and product molecules in the channels, resulting in the high activity. According to the above reaction mechanism, the byproduct Ar-H was formed mainly through a transition state of HCOO-Pd-Ar obtained via nucleophilic substitution of I-Pd-Ar with $HCOO^-$ [27]. Owing to the hydrophobicity of the catalyst resulting from the Ph-modification, less water molecules could entrance the channels, which may inhibit the dissociation of HCOONa to $HCOO^-$. Thus, the formation of HCOO-Pd-Ar species could be effectively inhibited, which reduced the side reaction and as a result, increased the selectivity to biphenyl.

The heterogeneous catalyst is preferable owing to the recyclability. It can be seen from Table 3 that Pd/Ph-MCM-41 catalyst was able to be used atleast three times with only slight decreases in the activity and selectivity. ICP-OES data revealed that the palladium content remained almost unchanged in the catalyst after the catalytic run and that palladium was undetectable in

Table 2
Influences of reaction temperature and time on the Ar-I Ullmann reaction

Temperature (°C)	Time (h)	Conversion (%)	Selectivity (%)	Yield (%)
80	10	70.6	99.1	70.0
100	10	75.4	98.0	73.8
120	10	81.6	94.6	77.2
100	12	88.4	87.9	77.7
100	14	86.3	86.3	74.4

Reaction conditions: 0.5 g 6 wt.% Pd/Ph-MCM-41 (1:4), 0.91 g Ar-I, 10 ml H_2O, 1.10 g HCOONa and 1.40 g KOH.

Table 3
Catalytic performance of various Pd-based catalysts on different supports and recycling tests of iodobenzene coupling reaction on Pd/Ph-MCM-41 (1:4)

Catalyst	Reaction times	Conversion (%)	Selectivity (%)	Yield (%)
Pd/SiO_2	1	27.0	26.0	7.0
Pd/MCM-41	1	65.3	52.4	34.2
Pd/Ph-MCM-41 (1:19)	1	71.8	90.8	65.2
Pd/Ph-MCM-41 (1:9)	1	73.4	94.2	68.2
Pd/Ph-MCM-41 (1:4)	1	75.4	98.0	73.8
	2	78.0	88.8	70.0
	3	74.1	85.7	63.5

Reaction conditions: 0.5 g catalyst with 6 wt.% Pd, 0.91 g Ar-I, 10 ml H_2O, 1.10 g HCOONa and 1.40 g KOH, reaction temperature = 100 °C, reaction time = 10 h.

the reaction product, implying that the amount of Pd dissolved from the Ph-MCM-41 support is neglected.

4. Conclusions

This study developed a new supported Pd catalyst (Pd/Ph-MCM-41) for the iodobenzene Ullmann reaction in aqueous conditions and supplied a powerful way to design clean organic synthesis by using water instead of organic solvent as reaction media. More specially, the following points are highlighted:

1. Pd/Ph-MCM-41 and Pd/MCM-41 showed higher activity and better selectivity than Pd/SiO_2, possibly owing to the high and uniform dispersion of Pd active sites and the ordered mesoporous structure.
2. Modifying MCM-41 with Ph-groups could further enhance the activity and selectivity owing to the increase in hydrophobicity of the catalyst which favored the entrance of iodobenzene molecules in the channels while inhibiting the entrance of water molecules. On one hand, it facilitated adsorption of reactant molecules on Pd active sites and thus enhanced the activity. On the other hand, it reduced the side reaction to form benzene by inhibiting the nucleophilic substitution to form HCOO-Pd-Ar, a key transition state to produce benzene during Ullmann reaction, and thus enhanced the selectivity to biphenyl.

Acknowledgements

This work was supported by the National Natural Science Foundation of China (20377031, 20407014 and 20521140450), Shanghai Municipal Scientific Commission (03DJ14005 and 03QF14037), Shanghai Municipal Educational Commission (04DB05) and Shanghai Leading Academic Discipline Project (T0402).

References

[1] G. Bringmann, R. Alter, R. Weirich, Angew. Chem. Int. Ed. Engl. 102 (1990) 1006.
[2] S. Svenkatraman, C.J. Li, Org. Lett. 1 (1999) 1133.
[3] M.R. Dack, J. Chem. Soc. Rec. 4 (1975) 211.
[4] Y. Zhang, D. Wang, Z.T. Huang, J. Prog. Chem. 11 (1999) 394.
[5] S. Zhang, D. Zhang, L.S. Liebeskind, J. Org. Chem. 62 (1997) 2312.
[6] J. Hassan, Chem. Rev. 102 (2002) 1360.
[7] A. Corma, Chem. Rev. 97 (1997) 2373.
[8] C.T. Kresge, M.E. Leonowicz, W.J. Roth, J.C. Vartuli, J.S. Beck, Nature 39 (1992) 710.
[9] S. Inagaki, S. Guan, T. Ohsuna, O. Terasaki, Nature 416 (2002) 304.
[10] D. Macquarrie, Chem. Commun. 77 (1996) 1961.
[11] K. Moller, T. Bein, Chem. Mater. 10 (1988) 2950.
[12] A.S. Maria Chong, X.S. Zhao, A.T. Kustedjo, S.Z. Qiao, Micropor. Mesopor. Mater. 72 (2004) 33.
[13] S.L. Burkett, S.D. Sims, S. Mann, Chem. Commun. 11 (1996) 1367.
[14] F. de Juan, E. Ruiz-Hitzky, Adv. Mater. 12 (2000) 430.
[15] H.Y. Huang, R.T. Yang, D. Chinn, C.L. Munson, J. Ind. Eng. Chem. Res. 42 (2003) 2427.
[16] H. Hata, S. Saeki, T. Kimura, Y. Sugahara, K. Kuroda, Chem. Mater. 11 (1999) 1110.
[17] P.T. Tanev, M. Chibwe, T. Pinnavaia, Nature 368 (1994) 321.
[18] R.H. Simon, E.F. Christabel, L. Benedicte, M. Stephen, Chem. Commun. (1999) 201.
[19] J.Y. Choi, C.H. Kim, D.K. Kim, J. Am. Ceram. Soc. 81 (1998) 1184.
[20] Y.D. Xia, W.X. Wang, R. Mokaya, J. Am. Chem. Soc. 127 (2005) 790.
[21] K. Moller, T. Bein, R.X. Fischer, Chem. Mater. 11 (1999) 665.
[22] S.J. Gergg, K.S. Sing, Adsorption, Surface Area and Porosity, 2nd ed., Academic, New York, 1982, p. 10.
[23] J. Beck, J. Vartuli, W. Roth, J. Am. Chem. Soc. 114 (1992) 10834.
[24] J. Panpranot, K. Pattamakomsan, P. Praserthdam, J. Phys. Chem. B 105 (2004) 6014.
[25] J. Panpranot, J.G. Goodwin, A. Sayari, J. Catal. Today 77 (2002) 269.
[26] A.C. Thomas, Photoelectron and Auger Spectroscopy, 1st ed., Plenum, New York, 1975, p. 352.
[27] W.H. Zhang, X.B. Lu, J.H. Xiu, Adv. Funct. Mater. 14 (2004) 544.